

QUT Digital Repository:  
<http://eprints.qut.edu.au/>



Rayment, Erin A. and Dargaville, Tim R. and Shooter, Gary K. and George, Graeme A. and Upton, Zee (2008) Attenuation of protease activity in chronic wound fluid (CWF) with bisphosphonate-functionalised hydrogels. *Biomaterials* 29(12):pp. 1785-1795.

© Copyright 2008 Elsevier

**Attenuation of protease activity in chronic wound fluid (CWF) with bisphosphonate-functionalised hydrogels**

Rayment, E.A.<sup>1\*</sup>, Dargaville, T.R.<sup>1</sup>, Shooter, G.K.<sup>1</sup>, George, G.A.<sup>1</sup>, Upton, Z.<sup>1</sup>

<sup>1</sup>Tissue Repair and Regeneration Program, Institute of Health and Biomedical Innovation, Queensland University of Technology, Brisbane, Queensland, Australia

\*Corresponding author: Erin Rayment, Tissue Repair and Regeneration Program, Institute of Health and Biomedical Innovation, Queensland University of Technology, 60 Musk Ave, Brisbane, Queensland, 4059, Australia. Email: [e.rayment@qut.edu.au](mailto:e.rayment@qut.edu.au)

**Short Title:** Bisphosphonate-functionalised hydrogels

Chronic ulcers are an important and costly medical issue, imposing considerable pain, reduced mobility and decreased quality of life. The common pathology in these chronic wounds is excessive proteolytic activity, resulting in degradation of key factors critical to the ulcer's ability to heal. Matrix metalloproteinases (MMPs), a large family of zinc-dependent endopeptidases, have been shown to have increased activity in chronic wound fluid (CWF), with many authors suggesting that they need to be inhibited for the ulcer to heal. The studies we report here show that the excessive MMP activity in CWF can be inhibited with the bisphosphonate alendronate, in the form of a sodium salt, a functionalised analogue, and tethered to a poly(2-hydroxy methacrylate) (PHEMA) hydrogel. Furthermore, these functionalised-alendronate hydrogels appear to be biocompatible as assessed in a three-dimensional *ex vivo* human skin equivalent model. Together, these results highlight the potential use of a tethered MMP inhibitor to inhibit protease activity in wound fluid. This approach may improve wound healing as it still allows MMPs to remain active in the upper cellular layers of the ulcer bed where they perform vital roles in wound healing; thus may offer an attractive new device-orientated wound therapy.

## 1. INTRODUCTION

Many current topical treatments for chronic ulcers have been designed to rectify the imbalance of growth-factors in the wound bed. One example is Regranex® from Johnson & Johnson, which delivers platelet-derived growth factor from a hydrogel dressing. While products like these introduce a positive flux of growth factors into the wound, they have been found to be only minimally effective [1]. Many authors have postulated that this is due to the excessively high levels of proteolytic activity, namely MMP activity, found in CWF [1-4]. In view of this, it has been suggested that the addition of a protease inhibitor prior to topical treatment of the wound may promote healing [3, 5-7]. There are a number of specific synthetic inhibitors of MMPs, namely tetracyclines and their chemically modified derivatives, e.g. doxycycline [6, 8, 9]; hydroxamic acids, e.g. GM6001 [10]; and bisphosphonates, e.g. clodronate [11]. The bisphosphonates are particularly appealing for use in chronic ulcers as they have been used clinically for a number of years to treat MMP-related disorders. Furthermore, they exhibit low toxicity and are therefore generally well-tolerated [12].

Bisphosphonates are small molecules, specifically referred to as geminal bisphosphonates when two C—P bonds are found on the same carbon atom [13]. Quite similar to endogenous pyrophosphates, bisphosphonates replace the O—P with a C—P, thereby allowing two additional functional groups [14], as well as creating a hydrolysis-resistant P—C—P bond [15]. In terms of MMP-inhibition, they are capable of binding to divalent metal ions, e.g.  $Zn^{2+}$ ,  $Ca^{2+}$  [16], through a three-dimensional structure that allows the coordination of one oxygen from the phosphate group with the cation [14]. This affinity for divalent cations can be increased even further if one of the functional groups is either a hydroxyl (OH) or a primary amine ( $NH_2$ ), as this then facilitates the formation of a tridentate conformation with the cation [14]. In addition, the nitrogen atom in the side chain must be in a particular spatial arrangement, as well as being a critical distance from the cation, for the bisphosphonate to be the most potent [17]. As a result, there has been a lot of work aimed at designing new and improved bisphosphonates in recent years, resulting in hundreds of new bisphosphonates being synthesised [17].

Bisphosphonates have been shown to inhibit MMP-1, -2, -3, -8, -9, -12, -13 and -20 at both therapeutically obtainable and, most importantly, non-cytotoxic concentrations [16]. Current clinical applications generally include the management of calcium and bone metabolism disorders, e.g. osteoporosis, Paget's disease, hypercalcaemia and metastatic cancer [15]. For a number of years now, these diseases have been effectively treated with bisphosphonates. Therefore, it appears that for future indications, including those primarily caused by significant soft tissue destruction, e.g. chronic ulcers, bisphosphonates may be a promising treatment [12]. In terms of chronic ulcer treatments, the delivery of specific bisphosphonates, or indeed simply the presentation of this particular chemical to the site of excessive protease activity, has to be carefully contemplated. This is due to more recent reports suggesting that the MMPs present in the ulcer environment may also be involved in other biological processes important to wound healing, such as growth factor activation and immune system regulation, rather than simply degrading the wound bed matrix and growth factors [18-21]. The goal of this study, which is significantly different from protease-inhibitory strategies proposed by others, is therefore to inactivate the proteases in the wound fluid after the fluid is absorbed away from the actual wound bed. In this situation the proteases required for healing-associated functions within the upper cellular layers of the wound bed remain available.

Bisphosphonates have previously been modified for clinical delivery, especially in terms of bone-specific applications [22-24]. In addition, alendronate is a prime candidate bisphosphonate for functionalisation as it contains a primary amine – a convenient chemical group that can be easily manipulated for conjugation into a polymer using already-established methods [24]. Through a nucleophilic acyl substitution reaction, an amine, present in the alendronate sodium salt form, can be reacted with a vinyl-containing acid halide [25] to produce an alendronate tethered to an unsaturated carbon group. This group then allows for further polymerisation into an established hydrogel system. The experiments reported herein focus on the details surrounding this preliminary alendronate condensation reaction, and then describe how this alendronate-methacrylate can be copolymerised into a PHEMA/PEG hydrogel system. Furthermore, this bioactive wound dressing is tested for efficacy against protease activity in CWF, and is assessed in further cell-based assays to confirm biocompatibility with a human *ex vivo* skin model.

## **2. MATERIALS AND METHODS**

### **2.1 Chemicals**

2-Hydroxyethyl methacrylate (HEMA,  $\geq 99\%$  GC, Sigma-Aldrich, St Louis, MO, USA) and methacryloyl chloride (Sigma-Aldrich) were distilled under reduced pressure immediately prior to use. Polyethylene glycol 20,000 (PEG, Sigma-Aldrich), peroxidase from horseradish (Sigma-Aldrich) and 2,2'-Azinobis [3-ethylbenzothiazoline-6-sulfonic acid]-diammonium salt (ABTS, Pierce Biotechnology, Rockford, IL, USA), alendronate sodium salt (Merck, San Diego, CA, USA) and 4-methoxy phenol (Sigma-Aldrich) were used as supplied under the manufacturers' instructions. All H<sub>2</sub>O used was double deionised by ion exchange (MilliQ, Millipore, Billerica, MA, USA).

### **2.2 Functionalisation of alendronate**

In a round-bottom flask, alendronate sodium salt (300 mg, 0.92 mmol) was dissolved in aqueous NaOH (148 mg, 3.70 mmol in 7.4 mL H<sub>2</sub>O) with 4-methoxy phenol to inhibit polymerisation. The solution was cooled in an ice-salt bath then freshly distilled methacryloyl chloride (120 mg, 1.15 mmol) and NaOH (111 mg, 2.768 mmol in 5.5 mL H<sub>2</sub>O) was added step-wise, maintaining the pH above 11. The reaction was stirred vigorously for 20 hours, then acidified with HCl to pH 7. The resulting product was evaporated to dryness using a rotary evaporator and extracted with chloroform (CHCl<sub>3</sub>) to remove any impurities. The water layer was then precipitated with N,N-dimethylformamide (DMF) to obtain alendronate-methacrylate.

### **2.3 Characterisation of alendronate-methacrylate through FT-NMR spectroscopy**

<sup>31</sup>P spectra were recorded using a 400 MHz NMR Spectrometer (Bruker, Germany) at room temperature in deuterated water (D<sub>2</sub>O). Spectra were analysed using MestReC Version 4.9.9.6 software (Mestrelab Research, Santiago de Compostela, Spain).

## **2.4 Wound fluid sample collection and preparation**

Chronic wound fluid (CWF) samples were obtained from consenting patients of the St. Luke's Nursing Services (Brisbane, QLD, Australia), suffering from chronic venous ulcers and undergoing compression therapy. Ethical approval to collect these samples was obtained from both the Queensland University of Technology (QUT) and St. Luke's Nursing Services. A standard wound fluid collection technique has been established and was carried out at the clinical site. Briefly, ulcers were washed with sterile water prior to collecting wound fluid, followed by the application of an occlusive dressing over the wound. Exudate accumulated under the dressing after 30 min to 1 h was recovered by washing with 1 mL of saline. The fluid was removed with 26G x 0.5" needle and syringes (Terumo Medical, Somerset, NJ, USA) and collected in 1.5 mL Protein LoBind tubes (Eppendorf, Hamburg, Germany). The wound fluid samples were centrifuged at 14,000 g for 10 min, then the supernatant was filtered using 0.45 µm cellulose acetate filters (Agilent Technologies, Wilmington, DE, USA). The protein content for all samples was quantitated and standardised using the BCA Protein assay kit (Pierce Biotechnology, Rockford, IL, USA). The samples were then sub-aliquoted and stored at -80 °C until further analysis.

## **2.5 Analysis of MMP-inhibition through incubation with the alendronate-methacrylate**

A pooled sample of CWF was run on Collagen Type I zymograms as previously described [26] using Collagen Type I (Sigma-Aldrich) at a final concentration of 0.5 mg/mL in 10% total acrylamide gels under non-reducing conditions. Briefly, electrophoresis was performed at 4 °C under Laemmli conditions [27]. The gels were then washed in 2.5% Triton X-100 for 30 minutes, then a further 60 minutes, prior to incubation in 50 mM Tris-HCl, 10 mM CaCl<sub>2</sub> and 50 mM NaCl at pH 7.6 for 24 hours at 37 °C, with the following exception. Alendronate-methacrylate (2 mM of the equivalent bisphosphonate segment of alendronate-methacrylate) and alendronate sodium salt (2 mM) were included in separate zymogram incubation buffers and the zymograms were incubated at 37 °C for 24 hours. The gels were then stained using 0.25% Coomassie brilliant blue R-250 (Bio-rad Laboratories, Hercules, CA, USA)

(40% methanol, 10% acetic acid) and destained appropriately (40% methanol, 10% acetic acid). Protease activity was visualised as clear (unstained) bands.

## **2.6 Analysis and quantitation of collagen zymography**

Gels were scanned using GeneSnap version 6.07 (SynGene, Cambridge, UK) and analysed using GeneTools version 3.07 to determine the molecular weight and quantitate the clear bands (SynGene). All quantitative analyses were performed using three separate gels per treatment and values were expressed as a relative % of the untreated sample, similar to previously published reports [28, 29].

## **2.7 Synthesis of hydrogels**

Aqueous solutions of distilled HEMA were prepared (50% water, 30% PEG and 20% HEMA) with a vehicle control without alendronate-methacrylate and two concentrations of alendronate-methacrylate (2 mM and 20 mM of the equivalent bisphosphonate segment of alendronate-methacrylate in the monomer solution) (*Table 1*). Solutions were then placed between two glass plates separated by a silicone gasket and purged with argon. Each mould was approximately 75 mm x 50 mm x 3 mm and filled with 10 mL of monomer solution. The moulds were then exposed to gamma-irradiation in a Gamma-cell 220 (Atomic Energy of Canada Ltd, Ottawa, Canada) using a Co<sup>60</sup> source at a rate of 3.25 kGy/h to give a total dose of 10 kGy (*Table 4.1*). The hydrogels were removed from their moulds and cut into 1 cm x 1 cm square pieces for further analysis.

## **2.8 Analysis of polymerisation through NIR FT-Raman Spectroscopy**

Non-irradiated and irradiated samples were analysed by a Perkin Elmer System 2000 NIR FT-Raman spectrophotometer (Perkin Elmer, Waltham, MA, USA). The hydrogel samples were placed into glass vials for spectroscopic analysis and the spectra were analysed using Grams/AI (Thermo Electron Corporation, Waltham, MA, USA).



## **2.9 Analysis of MMP-inhibition through incubation with the alendronate-functionalised hydrogels**

Similar to that described above, a pooled sample of CWF was analysed through Collagen Type I zymography with the following alteration. Alendronate-functionalised hydrogels were cut into small pieces and included in the incubation buffer, along with a blank and a non-functionalised hydrogel to act as a vehicle control, and then incubated at 37 °C for 24 hours. Collagen Type I zymograms were then analysed as described previously.

## **2.10 Skin collection**

Skin samples were collected from consenting patients undergoing breast or abdomen reductions at the St. Andrews and Wesley Hospitals, Brisbane, QLD, Australia. Human ethical approval was obtained from both the hospitals and the Queensland University of Technology. The skin samples were collected in sterile jars containing antibiotic/antimycotic solution containing 10,000 units of penicillin/mL, 10,000 µg of streptomycin/mL and 25 µg of amphotericin B/mL, with penicillin G, streptomycin sulfate and amphotericin B as antimycotic in 0.85% saline (Invitrogen, Carlsbad, CA, USA). These samples were processed within 12 hours following storage at 4 °C in Dulbecco's Modified Eagle's Medium (DMEM) containing antibiotics.

## **2.11 Primary keratinocyte cell cultures**

Primary skin keratinocytes were isolated as previously described [30] and expanded on a feeder layer of lethally irradiated 3T3 mouse fibroblast feeder cells (i3T3s) in Green's Media [31] that contained 10% foetal calf serum (FCS – Hyclone, Logan, UT, USA). Keratinocytes were grown for 7 days with the medium replaced every 3-4 days.

## **2.12 Preparation of a three-dimensional human skin epidermis equivalent model**

A human skin equivalent (HSE) model was used as previously described [30] with the following modifications. Following keratinocyte addition to the sterile stainless steel rings on top of the HSEs, the composites were incubated for 24 hours at 37 °C/5% CO<sub>2</sub>. After this period, the rings were removed and the composites were raised to the air-liquid interface by moving them onto stainless steel grids in 6-well plates (Nunc). The cultures were maintained for 5 days at 37 °C/5% CO<sub>2</sub> before the hydrogel treatments were applied.

## **2.13 Biocompatibility testing of hydrogels using the HSE model**

At five days post air-liquid interface culture, the alendronate-functionalised hydrogels were placed on top of the composite, along with “no treatment” and “non-functionalised” hydrogels as controls. These hydrogels were exposed to the composite for 7 days at 37 °C/5% CO<sub>2</sub>, with the media being replaced at 3 days. At completion of the treatment, samples of the composite model were fixed and paraffin-embedded using standard protocols for haematoxylin and eosin (H&E) histological analysis.

## **2.14 Immunohistochemistry**

Paraffin sections of the HSEs were cut (3 µm sections) and then deparaffinised in ethanol and xylene. Briefly, this involved sequential incubations with solutions of 100% xylene, 100% ethanol, 95% ethanol, 70% ethanol and distilled water. Sections were then probed separately for: keratin 1/10/11 (K1/10/11), a marker for cornification and squamous cell differentiation; p63 (RDI Research Diagnostics, Concord, MA, USA), a p53 analogue that identifies normal basal cells as opposed to malignant tumours; and cleaved caspase-3 (Cell Signaling Technology, Danvers, MA, USA), a critical mediator of apoptosis in mammalian cells. For slides that were probed for cleaved caspase-3, antigen unmasking was required before the blocking step. Briefly, the slides were incubated at 37 °C in 10 mM citrate buffer (pH 3.0) for 30 min, before proceeding as normal. After incubation with primary antibodies for K1/10/11 (1:400), p63 (1:100) and cleaved caspase-3 (1:100), the sections were

probed using a Dako Envision kit (Dako Denmark A/S, Glostrup, Denmark) as per the manufacturer's instructions, with the exception that phosphate buffered saline (PBS) was used instead of TBS. After antibody development of the labelled secondary antibody with the 3,3' diaminobenzidine (DAB) chromogen solution, all sections were counterstained with haematoxylin for 30 seconds and analysed using light microscopy.

### 3. RESULTS

#### 3.1 Synthesis and characterisation of alendronate-methacrylate

Following the identification of excessive MMP-9 levels in CWF as described in previous studies [32, 33], potential MMP inhibitors were considered for incorporation into a hydrogel wound dressing. The bisphosphonate alendronate was chosen as it has been used for a number of years in clinical practice [15] and possessed an easily modified primary amine. The primary amine in alendronate was reacted with methacryloyl chloride to form the amide along with a pendant vinyl group (*Figure 1A*). This unsaturated carbon then allowed for further polymerisation (*Figure 1B*) into an aqueous PHEMA:PEG hydrogel system. The  $^{31}\text{P}$  spectra of the methacrylated product, along with the original alendronate, are shown in *Figure 2*. All peaks have been assigned and further details of the spectrum are outlined in *Table 2*. In *Figure 2C* a second triplet is seen upfield of the first, which can be assigned to a dimer of the original alendronate-methacrylate formed through P—O—P bonds of the bisphosphonate groups (*Figure 3*), and not the starting product as shown by the shift upfield.

#### 3.2 Analysis of MMP-inhibitory action of alendronate-methacrylate

To analyse the alendronate-methacrylate, an activity assay was used to compare its MMP-inhibitory activity to that of the original alendronate. Through incubation of CWF with increasing concentrations of either the original or the alendronate-methacrylate, the proteolytic activity was revealed by the use of Collagen Type I (*Figure 4A-B*). This demonstrated that both forms of the alendronate are able to inhibit CWF samples 1-6 to varying degrees. Densitometry was used to quantify the reduction in proteolytic activity revealed by zymography and are represented graphically in *Figure 4C*. Quantitatively, both inhibitors were able to decrease the amount of Collagen Type I degradation, as compared to the untreated CWF samples ( $p < 0.01$ ). From this functional assay, it appears that the addition of the methacrylate group to alendronate still allows for inhibition of MMPs at a physiological temperature over 24 hours, although at a reduced level of function compared to the native form.

### 3.3 Preparation and characterisation of alendronate-functionalised hydrogels

Following successful inhibition of MMPs in CWF with the alendronate-methacrylate, polymerisation was required to form the functionalised wound dressing. Three sets of hydrogels were successfully synthesised according to the conditions outlined earlier (*Table 1, Figure 1B*). NIR FT-Raman Spectroscopy demonstrated that a total dose of 10 kGy of gamma irradiation induced complete polymerisation of the alendronate-methacrylate and HEMA monomer to its copolymer form (*Figure 5*). This was evident by the absence of a characteristic C=C band at  $1639\text{ cm}^{-1}$  in the irradiated samples when compared with the monomer mixture. The hydrogel sheets were then characterised using both a functional protease assay, along with exposure to a three-dimensional *ex vivo* skin model to determine biocompatibility.

### 3.4 Analysis of MMP-inhibitory action of alendronate-functionalised hydrogels

The alendronate-functionalised hydrogels were analysed using Type I Collagen zymography to determine if the tethered alendronate still demonstrated MMP-inhibitory action. The hydrogels were cut into small pieces and incubated with the zymograms containing the CWF, along with an untreated control. Collagen Type I zymography of the pooled CWF samples showed a large amount of protease activity in the untreated control (lane 1) (*Figure 6A*). However, when the hydrogel pieces were present, all three treatments showed a visible decrease in the amount of Collagen Type I degradation (lanes 2-4) (*Figure 6A*). When the treatments were analysed using densitometry to quantitate the relative decrease in protease activity, the GA10X hydrogel, i.e. the hydrogel containing 20 mM of alendronate-methacrylate, displayed the ability to significantly reduce Collagen Type I degradation as compared with the non-hydrogel treated control ( $p < 0.01$ ) (*Figure 6B*). These results suggest the tethered alendronate is still able to inhibit MMPs as shown through a functional assay.

### **3.5 Biocompatibility testing using a three-dimensional human skin equivalent**

A three-dimensional human epidermal skin equivalent model was used to assess potential toxicity effects from the alendronate-functionalised hydrogels as compared to the vehicle hydrogel. The various hydrogels were applied to the stratified skin models for a seven-day period, with histological and immunochemical staining carried out upon completion of the experiment. Treatments included the vehicle control of hydrogel G, along with the two alendronate-functionalised hydrogels, GA1X and GA10X. Histological analysis showed a haematoxylin-stained basal layer, with an eosin-stained cornified layer of relatively the same thickness throughout for all treatments (*Figure 7*). For the GA10X hydrogel minimal basal cells are apparent, along with increased numbers of nucleated cells in the cornified layer. Hydrogel G and GA1X also show some nucleated cells in the cornified layer, however, they do not appear to be as numerous. When the sections were probed for specific skin markers, keratin 1/10/11 and p63, and the apoptotic marker, cleaved caspase-3, hydrogel GA10X revealed a minimal amount of p63 immunoreactive basal cells, confirming the histological analysis. In the control and hydrogel G treatments, there is no visible immunoreactivity of cleaved caspase-3 with apoptotic cells. Similarly, minimal cleaved caspase-3 immunoreactivity is evident in samples exposed to its functionalised counterparts, GA1X and GA10X. This indicates that the synthesised hydrogels appear promising for potential wound dressing treatments.

#### 4. DISCUSSION

MMP-9 has been previously identified as an abundant protease present in CWF, and is likely to have a key role in degrading both the extracellular matrix and growth factors in the chronic wound environment. Hence, it is not surprising that current topical treatments of chronic ulcers with bioactives, i.e. growth factors, have proven to be only slightly effective in treating this condition [1]. In view of this, a specific MMP inhibitor, namely the bisphosphonate alendronate, was chosen as a potential clinical treatment to aid in neutralising the aggressive proteolytic chronic wound environment; the ultimate goal of this strategy being to modulate the ulcer towards a healing state. The bisphosphonate family, which exhibits low toxicity and has been well tolerated for several years of human use, seems to be the ideal candidate for MMP-related diseases [12]. The wound treatment explored in this study examined the use of bisphosphonates to inhibit MMP activity in CWF. Importantly, the approach described differs significantly from previous methods in that we proposed inactivation of the proteases in the wound fluid, after the fluid is absorbed away from the actual wound bed, so that proteases required for wound healing-related functions within the upper cellular layers of the wound bed remain available.

Alendronate was chosen as the MMP-inhibitor for inclusion into the hydrogel, primarily due to the fact that it contains both amine and hydroxyl functional groups, which together can enhance the bisphosphonate's affinity for divalent cations [14]. However, it first has to be modified to allow further polymerisation into the synthetic wound dressing. Because alendronate is insoluble in common organic solvents, a two phase Shotten-Baumann reaction was chosen to react an acid chloride with the amine of alendronate. This reaction is well characterised and allows high yields of amides, mainly due to the fact that they are able to successfully compete with other reactive species present [34]. Briefly, this is a two phase reaction with the acid chloride suspended in the water phase containing the amine compound. At the boundary of the two phases, the amine reacts with the acid chloride, thereby generating the desired product. The  $^{31}\text{P}$  spectra showed an additional phosphorus-containing species in the resulting product, possibly due to the dimerisation of two functionalised alendronate molecules through the  $-\text{OH}$  group on the phosphate. Similar dimerisation has been shown with a similar phosphate-containing molecule, i.e. ethylene glycol

methacrylate phosphate (MOEP) [35]. Following the reaction to modify alendronate, the resulting product was then copolymerised into a PHEMA hydrogel system. FT-Raman spectroscopy revealed a complete polymerisation, thereby ensuring that no functionalised alendronate could be released from the hydrogel.

Critically, we demonstrate that alendronate tethered to a hydrogel was able to significantly decrease the levels of Type I Collagen degradation in CWF as compared to the untreated control ( $p < 0.01$ ). Interestingly, the vehicle hydrogel, i.e. the hydrogel without the alendronate-methacrylate, was also able to inhibit MMP activity as revealed through the Collagen Type I zymography, but to a lesser degree than the most concentrated alendronate-functionalised hydrogel, GA10X. A possible explanation for this is the chemical composition of PHEMA itself, as it contains three oxygen atoms in its unit structure that are all available for chelation [36]. Further evidence for this hypothesis is that  $\text{Ca}^{2+}$  itself has a strong tendency to chelate to oxygen atoms [37]. Therefore, through the use of a “self-chelating” hydrogel support, the vehicle treatment (hydrogel G) has the ability to chelate the cations required by MMPs for their stability and catalytic activity, e.g.  $\text{Ca}^{2+}$ ,  $\text{Zn}^{2+}$ . This chelating ability is then disrupted by copolymerisation with the alendronate-methacrylate at the lowest concentration (hydrogel GA1X). Zainuddin *et al.* (2006) previously postulated that by reducing the number of available oxygen atoms, the chelating mechanism is thereby reduced, and may then prevent the chelation of metal ions with PHEMA. Furthermore, Chirila *et al.* (2007) report massive calcification of PHEMA, both *in vitro* in simulated body fluid and *in vivo* as subcutaneous implants [38]. However, when the highest concentration of alendronate-methacrylate is copolymerised into the system (GA10X), the chelating ability of alendronate alone is stronger than the PHEMA support and overcomes the decreased response seen with GA1X. Therefore, taken together, these results indicate that the alendronate is still available to inhibit the MMPs in the CWF, while not being released into the wound bed. This is a significant advance over topically applied inhibitors as it allows MMPs to remain active in the wound bed where they perform vital roles in growth factor activation and immune system regulation [18-21], yet at the same time the unwanted MMPs, those in the CWF, are absorbed into the hydrogel where they are inactivated.



Three-dimensional *ex vivo* skin models are a useful tool for evaluating topical products, as well as overcome a number of ethical and practical issues associated with animal studies [39]. Furthermore, 3D-stratified layers of human epidermal cells grown in culture systems *in vitro* have been shown to be useful in assessing skin irritation potential [40]. Following on from this, the experiments reported herein showed that there were minimal differences between the three treatments, i.e. the vehicle and two alendronate-functionalised hydrogels, in terms of impact on visible structure and effect on a range of skin cell surface expression markers on the HSE model. An interesting point to note is that with both wound dressing treatments, nucleated cells became visible in the previously anuclear cornified layer. We suspect that the application of a topical dressing to the skin equivalent model results in culture medium being absorbed into the dressing, and therefore converts the air-liquid interface of the 3D skin model to a liquid-liquid interface. This may then stimulate the keratinocytes to migrate faster through the cornified layers and produce a more immature phenotype. This particular behaviour has also been described in previous reports, where cells in a similar three-dimensional skin model did not completely differentiate when still covered with culture medium [41]. Indeed, this may well underlie the well accepted evidence that a moist wound environment is essential for optimal wound healing [42].

In terms of expression of skin cell surface markers, the HSEs exposed to the three hydrogel treatments appeared to be relatively similar when probed with the skin differentiation marker keratins 1, 10 and 11 and the basal cell marker, p63. The main difference observed between the HSEs exposed to the three treatments was that minimal immunoreactivity was observed with p63 in the GA10X hydrogel. This is likely to be alleviated by first washing the alendronate-functionalised hydrogels – thereby minimising the increased adhesive potential, or “stickiness”, of the phosphonate polymer component, such as that demonstrated in previous adhesion studies using human peripheral blood mononuclear cells [43]. Apoptosis in the keratinocytes in the HSE was also analysed by immunoprobng for cleaved caspase-3 – a major effector caspase that is specific for keratinocytes undergoing apoptosis and not just those undergoing terminal differentiation [44]. None of the three treatments showed large levels of immunoreactivity to this cell surface marker, which appears

promising for future clinical treatments, especially in terms of developing MMP-inhibiting, CWF-absorbing functionalised hydrogels.

## 5. CONCLUSION

Taken together, the results reported herein suggest this novel alendronate-functionalised hydrogel holds promise as a dressing treatment for chronic wounds. This is due to its ability to inhibit the excessive levels of MMPs in CWF, as well as its biocompatibility when exposed to a human *ex vivo* skin model. Of importance to the development of this wound dressing was the ability to attach a functional group to the alendronate sodium salt, which then allowed polymerisation into the hydrogel system. This was achieved through a Shotten-Baumann reaction of the primary amine of alendronate with methacryloyl chloride, which permitted high yields of the amide in a single-step reaction. Furthermore, we have demonstrated that the MMPs in CWF can be inhibited by the original bisphosphonate alendronate, the methacrylated-analogue, and in a tethered state, i.e. attached to a hydrogel support. This last point is critical to the development of a successful chronic ulcer wound dressing as it inhibits the MMPs in CWF, while still allowing those on the wound bed itself to perform their essential functions in wound healing, namely, activation of growth-promoting agents and immune system modulation.

## REFERENCES

1. Cullen B, Watt PW, Lundqvist C, Silcock D, Schmidt RJ, Bogan D, *et al.* The role of oxidised regenerated cellulose/collagen in chronic wound repair and its potential mechanism of action. *Int J Biochem Cell B* 2002;34(12):1544-1556.
2. Stadelmann WK, Digenis AG, Tobin GR. Physiology and healing dynamics of chronic cutaneous wounds. *Am J Surg* 1998;126(Suppl 2A):26S-38S.
3. Tarnuzzer RW, Schultz GS. Biochemical analysis of acute and chronic wound environments. *Wound Repair Regen* 1996;4(3):321-325.
4. Trengove NJ, Stacey MC, Macauley S, Bennett N, Gibson J, Burslem F, *et al.* Analysis of the acute and chronic wound environments: the role of proteases and their inhibitors. *Wound Repair Regen* 1999;7:442-452.
5. Wysocki AB, Kusakabe AO, Chang S, Tuan T-L. Temporal expression of urokinase plasminogen activator, plasminogen activator inhibitor and gelatinase-B in chronic wound fluid switches from a chronic to acute wound profile with progression to healing. *Wound Repair Regen* 1999;7(3):154-165.
6. Yager DR, Nwomeh BC. The proteolytic environment of chronic wounds. *Wound Repair Regen* 1999;7(6):433-441.
7. Cullen B, Smith R, McCulloch E, Silcock D, Morrison L. Mechanism of action of PROMOGRAN, a protease modulating matrix, for the treatment of diabetic foot ulcers. *Wound Repair Regen* 2002;10(1):16-25.
8. Ramamurthy NS, McClain SA, Pirila E, Maisi P, Salo T, Kucine AJ, *et al.* Wound healing in aged normal and ovariectomized rats: effects of chemically modified doxycycline (CMT-8) on MMP expression and collagen synthesis. *Ann NY Acad Sci* 1999;878:720-723.
9. Ramamurthy NS, Kucine AJ, McClain SA, McNamara TF, Golub LM. Topically applied CMT-2 enhances wound healing in streptozotocin diabetic rat skin. *Adv Dent Res* 1998;12:144-148.
10. Lund LR, Romer J, Bugge TH, Nielsen BS, Frandsen TL, Degen JL, *et al.* Functional overlap between two classes of matrix-degrading proteases in wound healing. *EMBO J* 1999;18(17):4645-4656.
11. Valleala H, Hanemaaijer R, Mandelin J, Salminen A, Teronen O, Monkkonen J, *et al.* Regulation of MMP-9 (gelatinase B) in activated human monocyte/macrophages by two different types of bisphosphonates. *Life Sci* 2003;73(19):2413-2420.
12. Teronen O, Heikkila P, Konttinen YT, Laitinen M, Salo T, Hanemaaijer R, *et al.* MMP inhibition and downregulation by bisphosphonates. *Ann NY Acad Sci* 1999;878:453-465.

13. Fleisch H. Bisphosphonates in bone disease: from the laboratory to the patient. 3 ed. New York: Parthenon Publishing Group; 1997.
14. Heymann D, Ory B, Gouin F, Green JR, Redini F. Bisphosphonates: new therapeutic agents for the treatment of bone tumors. *Trends Mol Med* 2004;10(7):337-343.
15. Vasikaran SD. Bisphosphonates: an overview with special reference to alendronate. *Ann Clin Biochem* 2001;38:608-623.
16. Heikkila P, Teronen O, Moilanen M, Konttinen YT, Hanemaaijer R, Laitinen M, *et al.* Bisphosphonates inhibit stromelysin-1 (MMP-3), matrix metalloelastase (MMP-12), collagenase-3 (MMP-13) and enamelysin (MMP-20), but not urokinase-type plasminogen activator, and diminish invasion and migration of human malignant and endothelial cell lines. *Anti-Cancer Drug* 2002;13:245-254.
17. Russell RGG, Rogers MJ. Bisphosphonates: from the laboratory to the clinic and back again. *Bone* 1999;25(1):97-106.
18. Suzuki M, Raab G, Moses M, Fernandez C, Klagsbrun M. Matrix metalloproteinase-3 releases active heparin-binding EGF-like growth factor by cleavage at a specific juxtamembrane site. *J Biol Chem* 1997;272:31730 - 31737.
19. McQuibban G, Butler G, Gong J, Bendall L, Power C, Clark-Lewis I, *et al.* Matrix metalloproteinase activity inactivates the CXC chemokine stromal cell-derived factor-1. *J Biol Chem* 2001;276:43503 - 43508.
20. Levi E, Fridman R, Miao H, Ma Y, Yayon A, Vlodavsky I. Matrix metalloproteinase 2 releases active soluble ectodomain of fibroblast growth factor receptor 1. *Proc Natl Acad Sci USA* 1996;93:7069 - 7074.
21. Gearing A, Thorpe S, Miller K, Mangan M, Varley P, Dudgeon T, *et al.* Selective cleavage of human IgG by the matrix metalloproteinases, matrilysin and stromelysin. *Immunol Lett* 2002;81:41 - 48.
22. Balas F, Manzano M, Horcajada P, Vallet-Regi M. Confinement and Controlled Release of Bisphosphonates on Ordered Mesoporous Silica-Based Materials. *J Am Chem Soc* 2006;128(25):8116-8117.
23. Uludag H, Yang J. Targeting Systemically Administered Proteins to Bone by Bisphosphonate Conjugation. *Biotechnol Prog* 2002;18(3):604-611.
24. Wang D, Miller S, Sima M, Kopeckova P, Kopecek J. Synthesis and Evaluation of Water-Soluble Polymeric Bone-Targeted Drug Delivery Systems. *Bioconjugate Chem.* 2003;14(5):853-859.
25. Otera J. Transesterification. *Chem Rev* 1993;93(4):1449-1470.

26. Gogly B, Groult N, Hornebeck W, Godeau G, Pellat B. Collagen zymography as a sensitive and specific technique for the determination of subpicogram levels of interstitial collagenase. *Anal Biochem* 1998;255(2):211-216.
27. Laemmli UK. Cleavage of structural proteins during the assembly of the head of bacteriophage T4. *Nature* 1970;227:680-685.
28. Cook H, Stephens P, Davies KJ, Harding KG, Thomas DW. Defective extracellular matrix reorganization by chronic wound fibroblasts is associated with alterations in TIMP-1, TIMP-2, and MMP-2 activity. *J Invest Dermatol* 2000;115(2):225-233.
29. Lerman OZ, Galiano RD, Armour M, Levine JP, Gurtner GC. Cellular dysfunction in the diabetic fibroblast: impairment in migration, vascular endothelial growth factor production, and response to hypoxia. *Am J Pathol* 2003;162(1):303-312.
30. Topping G, Malda J, Dawson R, Upton Z. Development and characterisation of human skin equivalents and their potential application as a burn wound model. *Primary Intention* 2006;14(1):14-21.
31. Chakrabarty KH, Dawson RA, Harris P, Layton C, Babu M, Gould L, *et al.* Development of autologous human dermal-epidermal composites based on sterilized human allodermis for clinical use. *Brit J Dermatol* 1999;141(5):811-823.
32. Yager DR, Zhang LY, Liang H-X, Diegelmann RF, Cohen KI. Wound fluids from human pressure ulcers contain elevated matrix metalloproteinase levels and activity compared to surgical wound fluids. *J Invest Dermatol* 1996;107:743-748.
33. Wysocki AB, Staianocoico L, Grinnell F. Wound fluid from chronic leg ulcers contains elevated levels of metalloproteinases MMP-2 and MMP-9. *J Invest Dermatol* 1993;101(1):64-68.
34. Kemp D, Vellaccis F. Acyl Derivatives. In: *Organic Chemistry*. New York: Worth Publishers Inc.; 1980. p. 368-369.
35. Suzuki S, Whittaker M, Grondahl L, Monteiro M, Wentrup-Byrne E. In vitro mineralization of soluble and cross linked phosphate polymers. In: *International Symposium of Polymeric Materials for Regenerative Medicine*; 2007; Montreal, Canada; 2007.
36. Zainuddin, Hill D, Whittaker A, Chirila T. In-vitro study of the spontaneous calcification of PHEMA-based hydrogels in simulated body fluid. *J Mater Sci* 2006;17(12):1245-1254.
37. Levine B, Williams R. *The Role of Calcium in Biological Systems*. Boca Raton: CRC Press; 1982.

38. Chirila TV, Zainuddin, Hill DJT, Whittaker AK, Kemp A. Effect of phosphate functional groups on the calcification capacity of acrylic hydrogels. 2007;3(1):95-102.
39. Tornier C, Rosdy M, Maibach HI. In vitro skin irritation testing on reconstituted human epidermis: Reproducibility for 50 chemicals tested with two protocols. *Toxicol in vitro* 2006;20(4):401-416.
40. Lawrence JN. Application of in vitro human skin models to dermal irritancy: a brief overview and future prospects. *Toxicol in vitro* 1997;11(3):305-312.
41. Ohsawa T, Maruyama I, Senshu T. Collateral occurrence of deimination of keratins with differentiation of an immortalized newborn rat keratinocyte cell line cultured at air-liquid interface. 1999;19(1):68-73.
42. Winter GD. Formation of the Scab and the Rate of Epithelization of Superficial Wounds in the Skin of the Young Domestic Pig. *Nature* 1962;193(4812):293-294.
43. Pietschmann P, Stohlawetz P, Brosch S, Steiner G, Smolen JS, Peterlik M. The effect of alendronate on cytokine production, adhesion molecule expression, and transendothelial migration of human peripheral blood mononuclear cells. *Calcified Tissue Int* 1998;63(4):325-330.
44. Xue M, Campbell D, Jackson CJ. Protein C is an autocrine growth factor for human skin keratinocytes. *J Biol Chem* 2007;282(18):13610-13616.

**Figure 1. Reaction schemes.**

(A) Condensation reaction of methacryloyl chloride and alendronate sodium salt.

(B) Gamma-induced polymerisation of HEMA and alendronate-methacrylate.

**Figure 2. FT-NMR  $^{31}\text{P}$  spectrum of alendronate-methacrylate.**

(A) Labelled schematic of alendronate-methacrylate.

(B)  $^{31}\text{P}$  spectrum of alendronate.

(C)  $^{31}\text{P}$  spectrum of alendronate-methacrylate.

**Figure 3. Potential structure of alendronate-methacrylate dimer.**

**Figure 4. Collagen Type I zymography demonstrating inhibition of protease activity present in wound fluid samples by alendronate sodium salt and its methacrylated-counterpart.**

(A) Lanes 1-6 are CWF samples 1-6 (500 ng); Lanes 7-12 are CWF samples 1-6 (500 ng) with 2 mM of alendronate (*A*) present in the incubation buffer at 37 °C for 24 hours.

(B) Lanes 1-6 are CWF samples 1-6 (500 ng); Lanes 7-12 are CWF samples 1-6 (500 ng) with 2 mM of alendronate-methacrylate (*functionalised A*) present in the incubation buffer at 37 °C for 24 hours.

(C) Relative levels of protease activity in pooled CWF samples treated with respective inhibitors. The MMP-specific inhibition of collagen degrading activity was represented quantitatively through densitometric analysis. Levels are shown as the % collagen degrading activity as compared to the untreated samples,  $\pm$  SEM (n=3). Statistical significance is relative to the untreated samples and shown as # (p<0.01) as determined by Tukey's test.

**Figure 5. Analysis of alendronate-functionalised hydrogels using NIR FT-Raman Spectroscopy.** Spectra indicate intensity/ Raman shift in  $\text{cm}^{-1}$ .

(A) Unirradiated  $\text{H}_2\text{O}$ :HEMA:PEG

(B) GA1X

Irradiated  $\text{H}_2\text{O}$ :HEMA:PEG:1X alendronate-methacrylate (10 kGy)

(C) GA10X

Irradiated  $\text{H}_2\text{O}$ :HEMA:PEG:10X alendronate-methacrylate (10 kGy)



**Figure 6. Collagen Type I zymography demonstrating inhibition of protease activity present in wound fluid samples by alendronate-functionalised hydrogels.**

**(A)** Lane 1 is the pooled CWF sample with no treatment in the incubation buffer. Lanes 2-4 are the same pooled CWF sample with polymer G, GA1X and GA10X (*Table 1*) respectively cut into small pieces and present in the incubation buffer at 37 °C for 24 hours.

**(B)** Relative levels of protease activity in pooled CWF samples treated with the respective hydrogels. The MMP-specific inhibition of collagen degrading activity was represented quantitatively through densitometric analysis. Levels are shown as the % collagen degrading activity as compared to the control sample,  $\pm$  SEM (n=3). Statistical significance is relative to the control sample and shown as # (p<0.01) as determined by Tukey's test.

**Figure 7. Histological and immunohistochemical analysis of an *ex vivo* human skin model following exposure to the alendronate-functionalised hydrogel.** From left to right the staining is: haematoxylin and eosin (H&E), keratin 1/10/11 (K1/10/11), p63 and cleaved caspase-3 (CC-3). The scale bar measures 20  $\mu$ m. Hydrogel treatments are defined in *Table 1*.

Sample ID	H <sub>2</sub> O (g)	HEMA (g)	PEG 20,000 (g)	Alendronate-methacrylate (mg)
G	5.0	2.0	3.0	-
GA1X	5.0	2.0	3.0	7.68
GA10X	5.0	2.0	3.0	76.80

**Table 1. Functionalised hydrogel formulations prepared for analysis as potential wound dressings**

Peak	ppm	Multiplicity, coupling constant (Hz)	Norm. Int	Identity
a,b	21.51	t, 12.7	1.00	P on alendronate-methacrylate, split by CH <sub>2</sub>
	21.43			
	21.35			
1	21.16	t, 11.8	0.35	P on alendronate-methacrylate dimer ( <i>Figure 3</i> ), split by CH <sub>2</sub>
	21.09			
	21.01			

**Table 2. Features of alendronate-methacrylate FT-NMR <sup>31</sup>P spectrum.** Columns are from left to right: peak number; shift (ppm); multiplicity (s, d, t, m) and coupling constant (Hz); normalised integral; and identity.

Figure 1

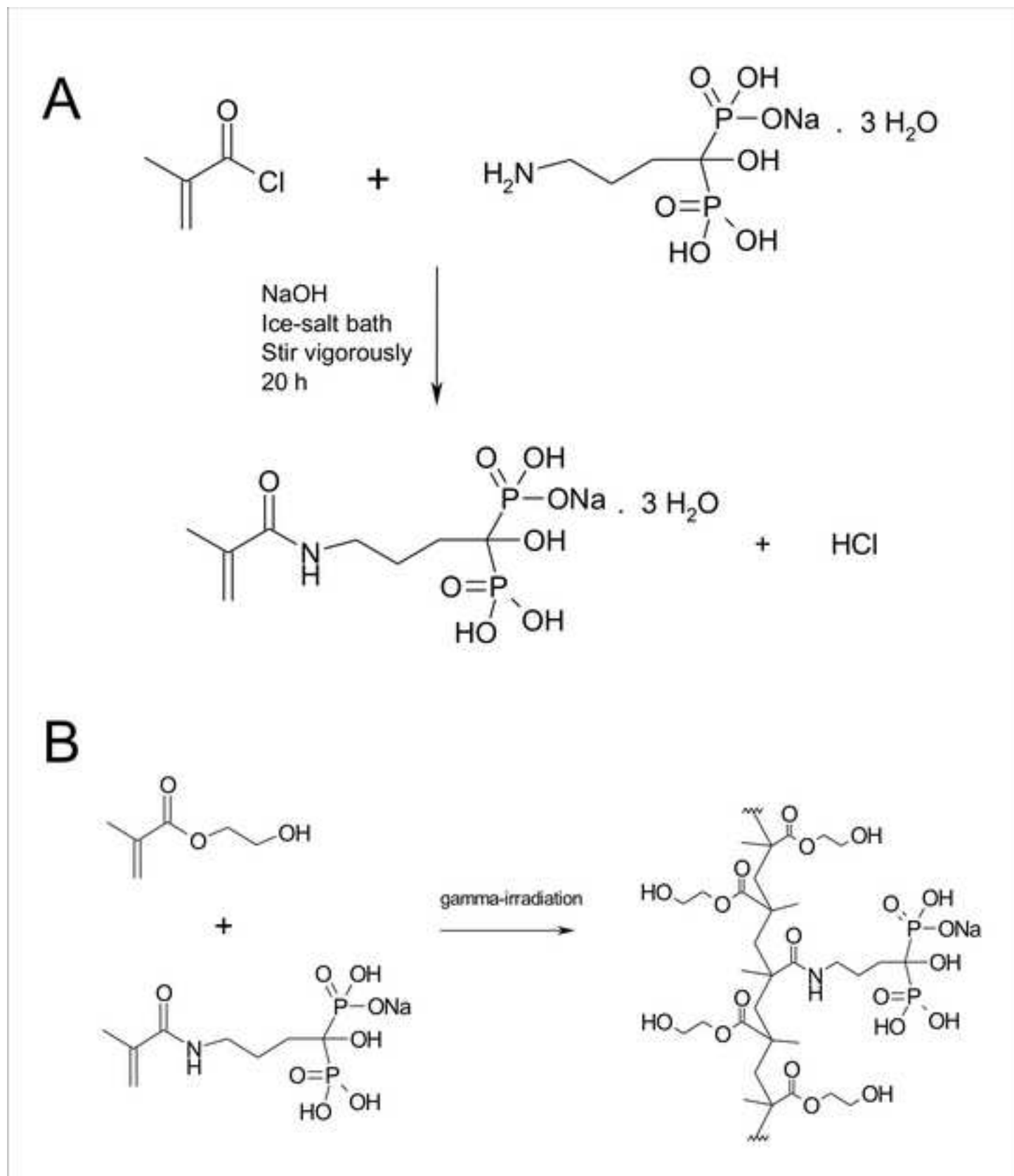
[Click here to download high resolution image](#)

Figure 2

[Click here to download high resolution image](#)

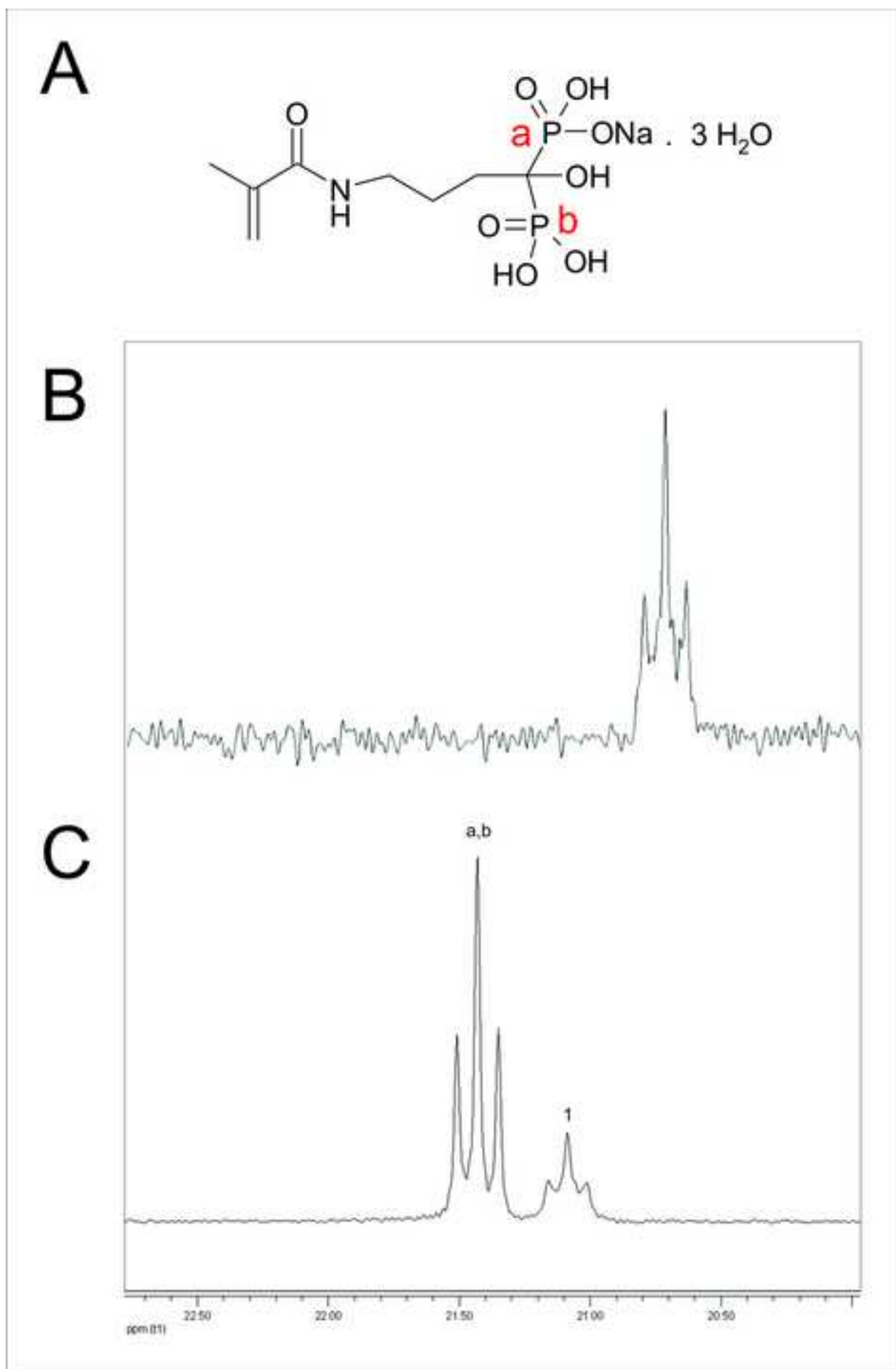


Figure 3  
[Click here to download high resolution image](#)

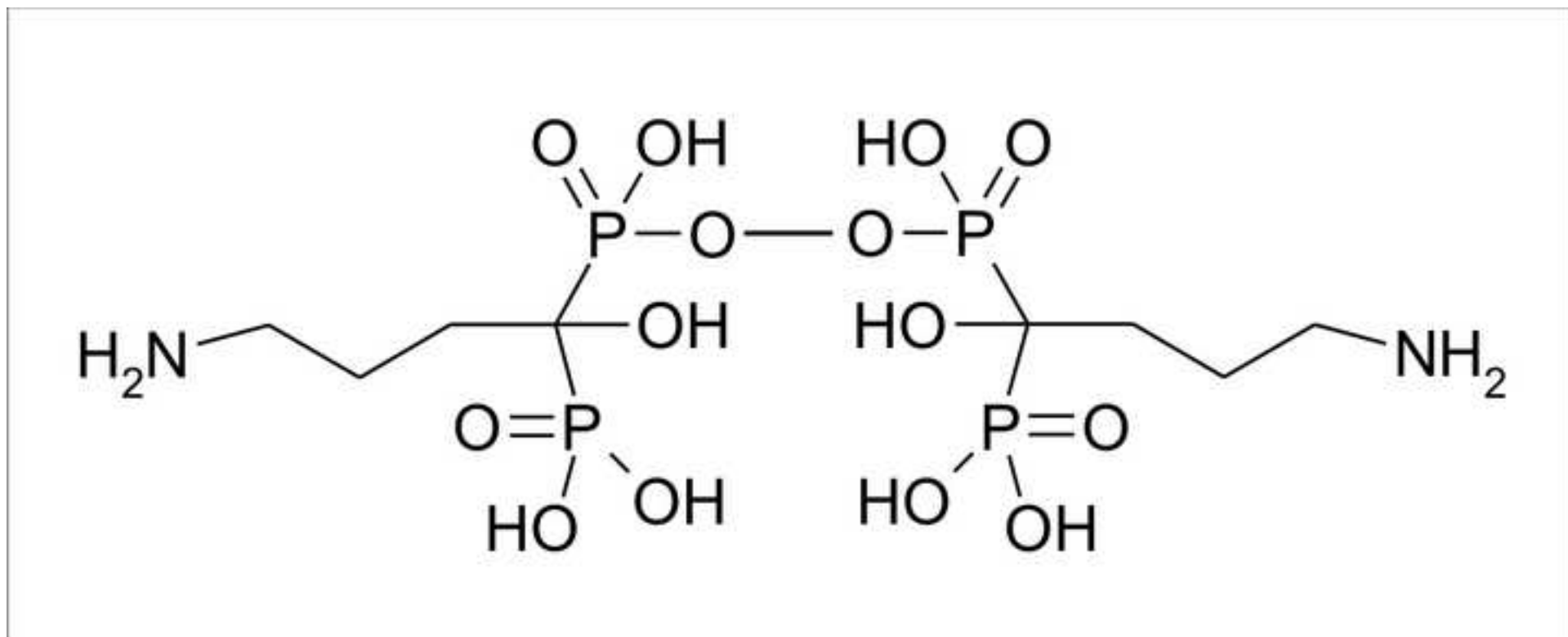


Figure 4  
[Click here to download high resolution image](#)

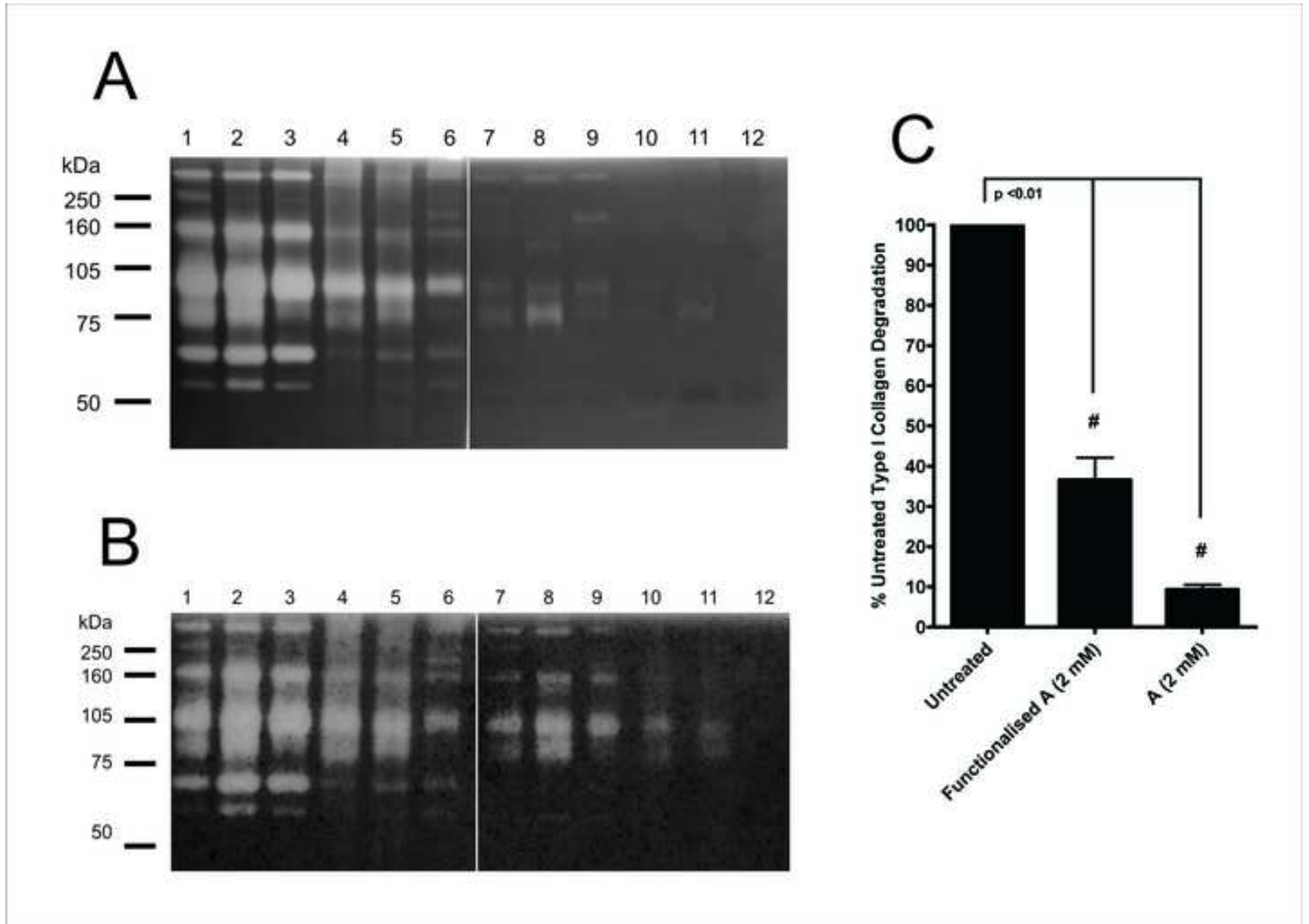


Figure 5  
[Click here to download high resolution image](#)

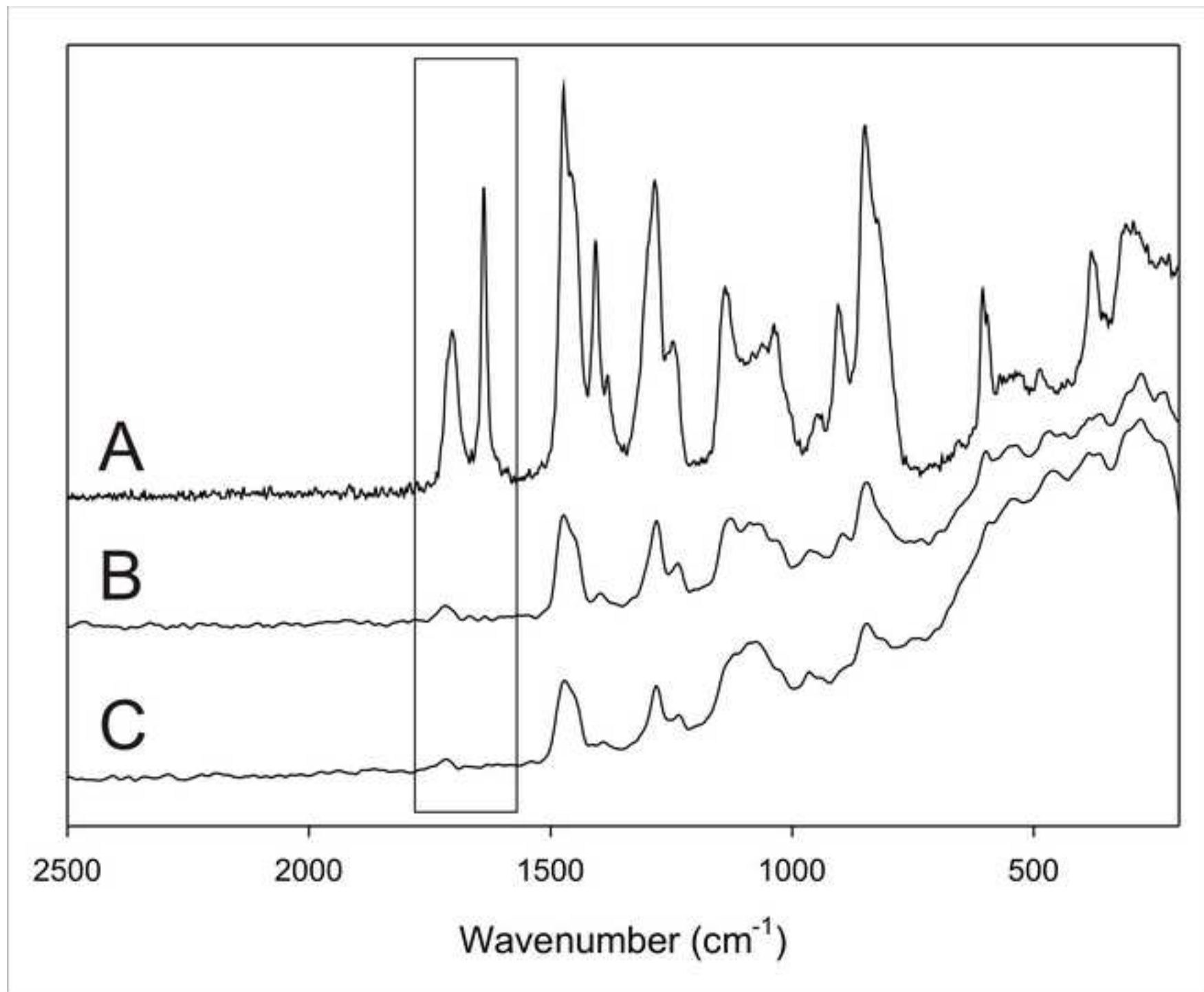


Figure 6  
[Click here to download high resolution image](#)

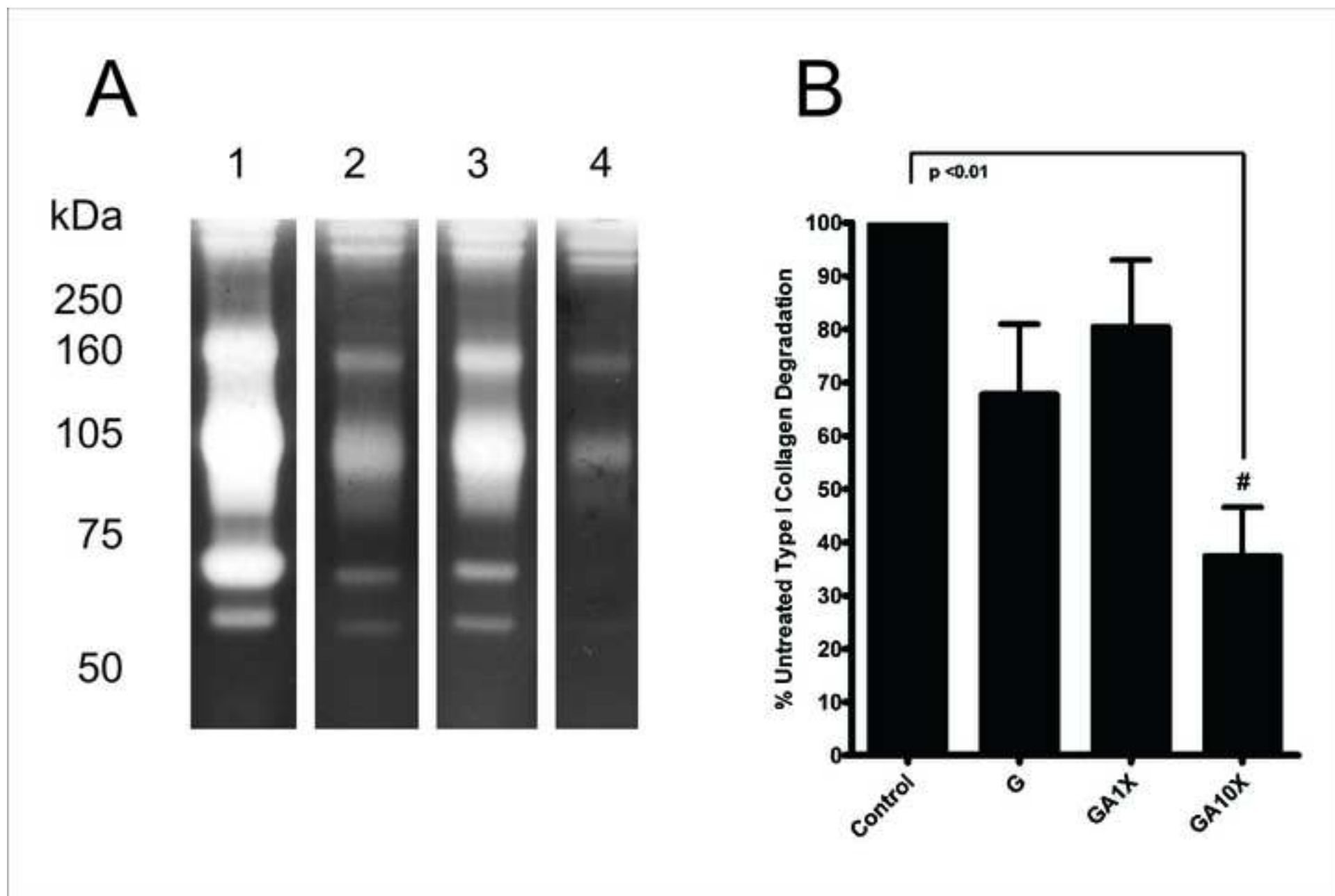




Figure 7  
[Click here to download high resolution image](#)

